Q. Rong
General Electric Corp.,
Cleveland, OH 44112

D. Ceglarek
Dept. of Industrial Engineering,
The University of Wisconsin—Madison,
Madison, WI 53706-1572
e-mail: Daeek@engr.wisc.edu

J. Shi
Dept. of Industrial and Operations Engineering,
The University of Michigan,
Ann Arbor, MI 48109
e-mail: shihang@umich.edu

Dimensional Fault Diagnosis for Compliant Beam Structure Assemblies

A model-based diagnostic methodology is proposed for the dimensional fault diagnosis of compliant beam structures in automotive or aerospace assembly processes. In the diagnosis procedure, the product measurement data are used to detect and isolate dimensional faults caused by part fabrication error in compliant beam assemblies. The proposed method includes a predetermined fault patterns model and a fault mapping procedure. The fault patterns are modeled by the diagnostic vectors derived from the inversed stiffness matrix of the beam structure. The fault mapping procedure combines principal component analysis (PCA) of measurement data and fault pattern recognition using statistical hypothesis tests. Verification of the proposed method is presented through simulations and one case study. [S1087-1357(00)02502-8]

1 Introduction

Increasing quality and productivity are two major goals in such high volume sheet metal assembly processes as the automotive body assembly. The dimensional integrity of an automotive body has tremendous impact on the quality of the final vehicle. Dimensional quality is a measure of conformance between the actual geometry of manufactured products and their designed geometry.

Traditional methods for quality improvement are primarily based on statistical analysis of the measurement data for product, which focuses on process inspection and process change detection rather than root cause determination. Those methods are not effective for the fault determination of complex systems with high-volume production such as automotive body assembly.

Fault diagnosis methods can improve quality by eliminating product nonconformance and can increase productivity by reducing the breakdown time of the tooling. These methods can also reduce the ramp up time during the launch of a new process and product by eliminating preproduction faults.

Fault diagnosis approaches can be divided into heuristic-based diagnostics, evolutionary computation-based diagnostics, and model-based diagnostics methods [1]. Heuristic approaches, such as a rule-based approach, perform diagnosis based on the process knowledge collected from historical data. A number of successful industrial applications have been developed for mature production processes. However, they cannot be applied during a new product and process launch or during preproduction stages when historical data about the faults are unavailable. Evolutionary computation-based diagnostic approaches such as neural networks and genetic algorithms have strong abilities for learning a new fault configuration. However, they require a large amount of training data with varied fault patterns, and thus cannot be applied during the launch of a new product. Model-based fault diagnostic systems generally use diagnostic models to define the relationship between the measured signals and individual faults [2]. The effectiveness of model-based diagnosis strongly depends on the correctness and comprehensiveness of the process and product models used for the diagnosis. In model-based diagnostic approaches, the diagnostic models have an analytical foundation; therefore, they can take advantage of various parametric identification and statistical techniques [3]. In the area of sheet metal assembly, there is only limited development in modeling of sheet metal processes and products for the purpose of fault diagnosis.

Tight quality and productivity requirements put great emphasis on the need of integrating in-line measurements (instead of off-line measurements) and in-process quality improvement (instead of post-process inspection). *In-Process Quality Improvement (IPQI)* focuses on the combination of process variability identification, localization, and root cause isolation of multi-level automotive body assembly systems. A hierarchical group structure model was developed to represent a multi-level body assembly system, and a statistical data grouping and diagnostic reasoning technique was developed based on this model. This modeling approach and its associated statistical analysis methods led to the first knowledge-based diagnosis methodology for dimensional control of the body assembly process [4]. Researchers have also focused on the fixture-failure-related problems in the assembly processes. A systematic methodology for single fault isolation of fixturing sheet metal assembly processes was developed by Ceglarek and Shi [5]. This method was expanded to include the multiple fault situation by using least square algorithms [6]. Rong and Bai [7] presented an analytical approach to study the locator error effect on part geometry accuracy by modeling three locating reference planes using geometric plane constraints. Recently, progress has also been made in modeling the variation propagation of multiple parts and multiple stations using a state space model [8]. All these approaches have significantly improved the understanding of fixture failures and diagnosis of sheet metal assembly processes. However, these approaches are based on the assumption that all assembled parts are rigid.

In sheet metal assembly processes, dimensional problems resulting from the compliant characteristics of the parts/subassemblies greatly impact the dimensional quality of the product. Shalon et al. [9] and Shiu et al. [10] indicated that part deformations due to the compliant characteristics are among one of the most frequent causes of preproduction dimensional problems.

This paper will focus on the diagnosis of dimensional faults of sheet metal assemblies, considering the compliant characteristics of the parts/subassemblies. Little work has been done on the diagnosis of compliant assembly processes. The presented methodology is based on the beam-based modeling of assembly structures developed by Shiu et al. [10] and on the in-line dimensional measurements of the products. A generic model of dimensional faults for compliant beam structure assemblies is developed in the form of diagnostic vectors. Diagnostic vectors are derived from the inversed stiffness matrix of the beam structure. On the other

Contributed by the Manufacturing Engineering Division for publication in the JOURNAL OF MANUFACTURING SCIENCE AND ENGINEERING. Manuscript received July 1998; revised Oct. 1999. Associate Technical Editor: E. DeMeter.

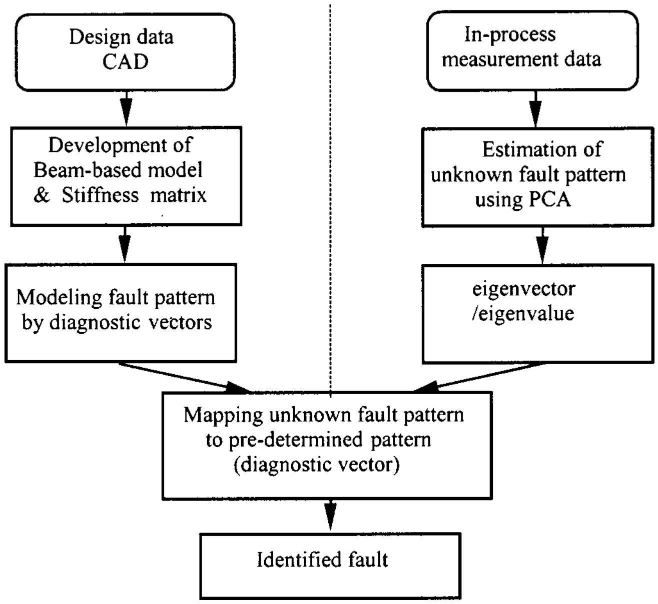

Fig. 1 The structure of the diagnostic methodology

hand, fault symptoms (variation patterns) obtained from the measurement data are modeled using principal component analysis (PCA), as eigenvalue/eigenvector pairs. The analytical relationship between engineering model (the diagnostic vector) and statistical model (the fault pattern) is established, which lays the basis of scientific understanding and application of the PCA in the diagnosis of compliant assemblies. The fault mapping is executed using pattern recognition and statistical hypothesis tests as decision criteria. The outline of this approach is shown in Fig. 1.

This paper is organized as follows. The assembly process, fault-symptom relation and beam-based modeling method for compliant beam structures are described in Section 2. In Section 3, a generic model of dimensional faults in the form of diagnostic vectors is developed. The analytical relationship between diagnostic vectors and fault patterns obtained from the measurement data represented by the eigenvalue/eigenvector pairs is derived. In the last part of Section 3, the diagnostic reasoning and fault mapping procedure is developed using statistical hypothesis tests. To illustrate the proposed method, simulation results and a case study are presented in Sections 4 and 5 respectively. Conclusions are summarized in Section 6.

2 Assembly Process Modeling

2.1 Assembly Process of Compliant Parts. Compliant assemblies are widely used in automotive body and airplane frame manufacturing industry. The assembly processes for compliant parts are very complex and these products require high dimensional accuracy in general. For example, an automotive body is assembled out of 200–300 sheet metal parts and subassemblies in 55–75 assembly stations (fixtures), and the dimensional accuracy of the body needs to be controlled within 2 mm (6 sigma product-to-product variation) in order to meet the functional requirements of the vehicle [11]. The automotive assembly process is monitored by measuring certain selected locations on the body assembly and subassemblies. There is no approach that is able to monitor the tooling elements or part joints directly. The fault diagnosis is conducted with the measurement data of the products. Usually, the product dimensions are measured with an in-line optical coordinate measurement machine (OCMM). Measurement locating points (MLPs) for monitoring key product and process characteristics are selected at different locations on the body according to importance and requirements. An automotive body usually has 100 to 150 MLPs monitoring the *X*, *Y*, and *Z* coordinates on major subassemblies at different manufacturing stages throughout the assembly process. The measurement information has a multivariate nature, which reveals the dimensional conditions at different locations on the whole body structure. Figure 2 shows an example of the MLPs layout on the final stage of the automotive body assembly. While the multivariate measurements are able to indicate the dimensional conditions at different MLPs, they cannot provide any direct information related to the sources (dimensional faults) of the dimensional problems. Thus, it is necessary to extract the variation patterns from the multivariate measurement data for fault diagnosis. The variation patterns represent the interrelationship among the multiple variables on the body structure and manifest the symptoms of the faults.

2.2 Fault-Symptom Relation and Hypothetical Dimensional Fault Domain. Dimensional problems are defined as the nonconformance of product dimensions to its designed values. Dimensional problems of automotive body assembly can be two fold in nature and can manifest themselves as dimensional deviations and dimensional variations. Dimensional deviation measures the difference between product feature or characteristic and its designed nominal. Dimensional variation measures the dispersion of a product feature or characteristic among a set of products or parts. Variation is a statistical index that examines the degree of consistency of different product units and the stability of the process. According to quality control theories, for nominal-the-best processes, a two-step procedure is often employed: (1) reduce the dispersion (variation), and (2) move to the nominal (reduce the deviation). Step (1) is more challenging.

In the automotive body assembly process, unit-to-unit variations are among the most frequently occurring dimensional problems. When a manufacturing process is working properly, the variations indicate the random nature of the process; when faults occur, excessive variations reveal the presence of dimensional faults. There are no simple ways to control variations, a comprehensive diagnostic approach that integrates multivariate statistics with information about the product and process design must be employed.

Dimensional variation can be caused by (1) part misalignment (lack of part locating stability); and (2) deformation by

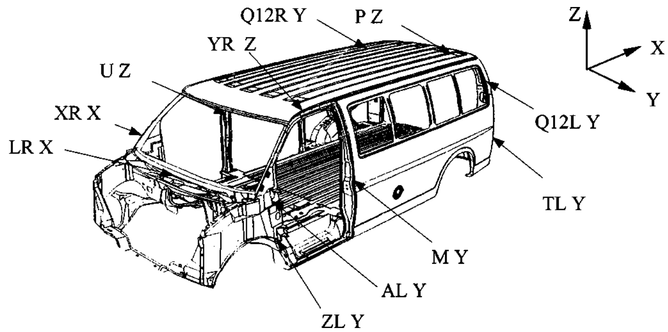

Fig. 2 An example of the measurement locating point layout on the automotive body

part-to-part interferences resulting from part fabrication errors [12]. The latter enables us to consider the compliant characteristics of sheet metal assemblies. The diagnosis of dimensional variation caused by part misalignment for rigid fixtures were described in Ceglarek and Shi [5] and Apley and Shi [6]. However, there is no method to diagnose the faults of part-to-part interferences.

In this paper, we will focus on the diagnosis of dimensional variation of compliant assemblies. The fault is defined as any part-to-part interferences resulting from part fabrication errors. Considering the compliant characteristics of assemblies, the location of fault and the layout of product design will determine the deformation modes of the assemblies which manifest themselves as different variation patterns from the product measurement data.

In real assembly processes, it is reasonable to assume that one dominant fault exists at a time (for one particular assembly station). Generally, there are always more than one tooling element and part-to-part joint in an assembly station. It is possible that two faults occur simultaneously. The single-fault-at-a-time assumption is based on the fact that the dominant fault contributes the most to the total variation. Furthermore, based on the design principle of assembly fixturing which requires tooling elements to be independent of each other, there is small probability that two or more faults occur simultaneously. From a diagnosis and process control point of view, if one fault occurs, it should be eliminated right away. If the diagnostic performance is not effective and the fault cannot be eliminated on time, multiple fault situations may occur. In this situation, recursive steps of diagnosis are required. In this paper, a single fault at a time is assumed. All other factors including any possible nondominant simultaneous faults, unmodeled terms and measurement errors are treated as noise.

2.3 Beam-based modeling. The compliant characteristics of sheet metal are modeled by beam-based model. In the literature, Chon et al. [13] and Shiu et al. [10] applied the beam structure to model sheet metal assembly products. In the modeling procedure [10], the automotive body is decoupled into beam elements which represent the functional and structural requirements of the automotive parts. A simplified beam structure of the automotive body is shown in Fig. 3. The beam-based modeling approaches for both strength analysis and dimensional control of sheet metal assemblies have been shown to be effective. Chon et al. [13] reported a 95 percent accuracy for the beam-model of vehicle body structure stiffness when compared to real experimental testing results.

The beam-based modeling method in Fig. 3 includes the critical characteristics of the assembly process, such as all fixture locating and holding layout as well as the geometry of part-to-part joints. This allows the model to describe the deformations of parts and subassemblies caused by part-to-part interferences resulting from part fabrication errors. The basic elements of the beam-based model are nodes and beam members. Information in this beam structure model includes: (1) the position and direction of fixture locators, (2) the part-to-part joints (beam-to-beam joint), and (3) the measurement locating points on each beam member.

In the beam-based model, all dimensional faults are manifested by the deformations of the structure. These deformations are caused by structural forces, which are the results of part-to-part interferences during assembly process.

Based on the structure theory [14], the deformations of a structure are determined only when the structure is stably located. In general, this requirement is satisfied in the part/subassembly fixturing conditions where the N-2-1 locating schemes are used. The relationship between the structure deformations and structural forces is given by

$$\mathbf{X}=\mathbf{K}^{-1}\cdot\mathbf{P} \tag{1}$$

where $\mathbf{P}=(p_1,p_2,\ldots,p_n)^T$ represents the vector of total structure forces, and n is the number of nodes on the beam structure,

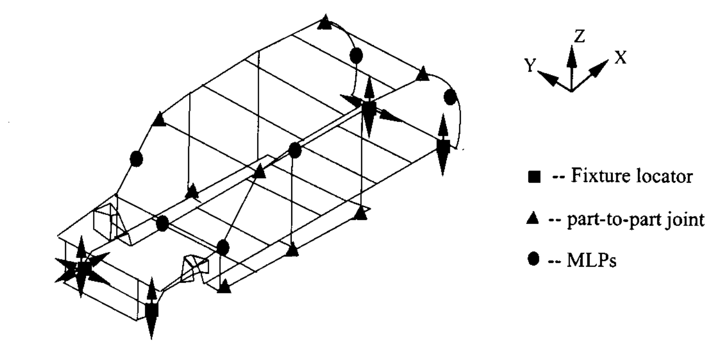

Fig. 3 The beam structure of an automotive body

$\mathbf{X}=(x_1,x_2,\ldots,x_n)^T$ is the vector of displacements at the corresponding measurement locating points on the structure, and $\mathbf{K}$ is the structure stiffness matrix consisting of n by n matrices and can be presented in the following form:

$$\mathbf{K}=\begin{bmatrix} K_{11} & K_{12} & \cdots & K_{1n} \\ K_{21} & K_{22} & \cdots & K_{2n} \\ \vdots & \vdots & \cdots & \vdots \\ K_{n1} & K_{n2} & \cdots & K_{nn} \end{bmatrix} \tag{2}$$

where $K_{ii}=\Sigma_{j=1}^{r}\beta_{ij}^{T}k_{ii}^{j}\beta_{ij}$, $K_{ij}=\beta_{ij}^{T}k_{ij}\beta_{ji}$, k_{ii} and k_{ij} are the beam member stiffness matrices, and β_{ij} and β_{ji} are compatibility matrices. The details of the derivations of k_{ii}, k_{ij}, β_{ij} and β_{ji} can be found in West [14] and Shiu et al. [10].

3 Diagnostics of Dimensional Faults Using Inversed Stiffness Matrix (ISM)

In this section, the analytical relationship between the modeled variation patterns and the statistical variation patterns from dimensional measurements will be established, and this relationship is the basis for the fault diagnosis.

The ISM-Diagnostic method is based on the diagnostic vectors derived from the Inversed Stiffness Matrix of the compliant beam-based structure model presented in Section 2.

3.1 Diagnostic Vectors. By decoupling the inversed stiffness matrix in Eq. (1) as

$$\mathbf{X}=\mathbf{d}(1)\cdot p_1+\mathbf{d}(2)\cdot p_2+\cdots+\mathbf{d}(i)\cdot p_i+\cdots+\mathbf{d}(n)\cdot p_n \tag{3}$$

we define $\mathbf{d}(i)=(d_{1i},d_{2i},\ldots,d_{ni})^T$ as a diagnostic vector which is the ith column vector of the inversed stiffness matrix $\mathbf{K}^{-1}$. From the beam-based model, the diagnostic vector $\mathbf{d}(i)$ ($i=1,2,\ldots,n$) is a constant vector, which is determined by the properties of the beam-structure, and measures the effect of the ith fault on $\mathbf{X}$. Equation (3) indicates that the displacement at a certain location on the assembly structure is the superimposition of the deformations caused by each individual fault that occurred. In addition, the variation pattern of the assembly caused by a given fault is solely determined by the diagnostic vector corresponding to that fault.

Under the single fault assumption, the relationship is reduced to

$$\mathbf{X}=\mathbf{d}(i)\cdot p_i \tag{4}$$

Equation (4) shows that the variation pattern of the modeled structure is determined by the corresponding diagnostic vector $\mathbf{d}(i)$, if only the ith fault occurs.

3.2 Description of Variation Pattern Using PCA. The faults in the actual assembly process are manifested through the measurements at the MLPs. While the measurement data can indicate dimensional problems occurring, they do not directly relate to the faults that cause these dimensional problems. In order to perform diagnosis, the variation patterns of the MLPs need to be extracted from the covariance of the multivariate measurement data. Previous research [5] proved that the variation patterns of the automotive body assembly can be estimated based on principal component analysis (PCA). By using PCA, the original set of variables are transformed into a new set of uncorrelated variables which account for most of the variance of the original covariance structure and measure the variation patterns of the data. The principal components and the original variables have the following relationship [15]

$$\mathbf{Z}=\mathbf{A}^T\cdot\mathbf{X} \tag{5}$$

where $\mathbf{Z}=(z_1,z_2,\ldots,z_j,\ldots,z_n)^T$ is the vector of principal components, $\mathbf{X}=(x_1,x_2,\ldots,x_j,\ldots,x_n)^T$ is the vector of original variables, $\mathbf{A}$ is the matrix of eigenvectors of the covariance matrix $\mathbf{S}$ of the original variables, and the jth column vector of $\mathbf{A}$, $\mathbf{a}_j=[a_{1j},a_{2j},\ldots,a_{nj}]^T$, is the jth eigenvector. $\mathbf{a}_j$ represents the variation pattern of the jth principal component.

According to the PCA, the covariance of the original variables can be represented by the eigenvalues and eigenvectors as

$$\mathbf{S}=\lambda_1\cdot\mathbf{a}_1\cdot\mathbf{a}_1^T+\lambda_2\cdot\mathbf{a}_2\cdot\mathbf{a}_2^T+\cdots+\lambda_n\cdot\mathbf{a}_n\cdot\mathbf{a}_n^T \tag{6}$$

where λ_j is the eigenvalue corresponding to the jth principal component, which accounts for the variance explained by the jth principal component.

For a single fault, the variation can be explained by the first eigenvalue/eigenvector pair $(\lambda_1,\mathbf{a}_1)$. Thus, Eq. (6) can be reduced to

$$\mathbf{S}=\lambda_1\cdot\mathbf{a}_1\cdot\mathbf{a}_1^T \tag{7}$$

The standard deviation of the original variables $\mathbf{X}$ is

$$\begin{bmatrix}\sigma_{x_1}\\ \sigma_{x_2}\\ \cdots\\ \sigma_{x_n}\end{bmatrix}=\begin{bmatrix}\sqrt{\lambda_1}a_{11}\\ \sqrt{\lambda_1}a_{21}\\ \cdots\\ \sqrt{\lambda_1}a_{n1}\end{bmatrix} \tag{8}$$

Equation (8) shows that the variation pattern of vector $\mathbf{X}$ is determined by eigenvalue/eigenvector pair $(\lambda_1,\mathbf{a}_1)$.

3.3 The Relationship Between the Diagnostic Vector and the Eigenvector/Eigenvalue of PCA. The deformation mode (variation pattern) of the modeled structure is determined by the diagnostic vectors $\mathbf{d}(i)$, as indicated in Eq. (4). The fault variation patterns can be described by the eigenvalues/eigenvectors of PCA based on the in-line measurement data. The analytical relationship between diagnostic vector and the eigenvalue/eigenvector pair is established here.

Theorem: A single fault, defined by the diagnostic vector $\mathbf{d}(i)$ based on the beam structure stiffness matrix (Eq. 2), is manifested through a variation pattern of a set of measurement points $(x_1,x_2,\ldots,x_n)^T$, and is described by one eigenvalue/eigenvector pair $(\lambda_1,\mathbf{a}_1)$, which has the relation $\mathbf{a}_1=\mathbf{d}(i)$.

Proof: From Eq. (8), the total standard deviation of the measurement data set is

$$\sigma=\sqrt{\lambda_1}\cdot\sqrt{\sum_{j=1}^{n}a_{j1}^2} \tag{9}$$

From the diagnostic vectors and Eq. (4), the total standard deviation can be calculated as

$$\sigma=\sqrt{\sum_{j=1}^{n}\sigma_{x_j}^2}=\sqrt{\sum_{j=1}^{n}d_{ji}^2\cdot\sigma_{p_i}^2}=\sigma_{p_i}\sqrt{\sum_{j=1}^{n}d_{ji}^2} \tag{10}$$

where σ_{p_i} is the standard deviation of the ith fault.

Again, from Eq. (4), the covariance matrix $\mathbf{S}$ is equal to

$$\begin{aligned}\mathbf{S}&=E[\mathbf{X}\mathbf{X}^T]=E[(\mathbf{d}(i)p_i)(\mathbf{d}(i)p_i)^T]\\ &=\mathbf{d}(i)E[p_ip_i^T]\mathbf{d}(i)^T=\sigma_{p_i}^2(\mathbf{d}(i)\mathbf{d}(i)^T)\end{aligned} \tag{11}$$

Based on Eq. (11)

$$\mathbf{S}\cdot\mathbf{d}(i)=\sigma_{p_i}^2(\mathbf{d}(i)\mathbf{d}(i)^T)\mathbf{d}(i) \tag{12}$$

Notice that

$$\sum_{j=1}^{n}d_{ji}^2=\mathbf{d}(i)\mathbf{d}(i)^T \tag{13}$$

From Eqs. (10) and (13), Eq. (12) can be represented as

$$\mathbf{S}\cdot\mathbf{d}(i)=\sigma^2\cdot\mathbf{d}(i) \tag{14}$$

From Eq. (9), Eq. (14) can be arranged as

$$\mathbf{S}\cdot\mathbf{d}(i)=\lambda_1\cdot\mathbf{d}(i)\cdot\sum_{j=1}^{n} a_{j1}^2 \tag{15}$$

Since eigenvectors $\mathbf{a}_1, \mathbf{a}_2, \ldots, \mathbf{a}_n$ are orthonormal, so we have

$$\mathbf{a}_1^T\cdot\mathbf{a}_1=\sum_{j=1}^{n} a_{j1}^2=1 \tag{16}$$

So, Eq. (15) is

$$\mathbf{S}\cdot\mathbf{d}(i)=\lambda_1\cdot\mathbf{d}(i) \tag{17}$$

which is equivalent to the definition of eigenvector $\mathbf{a}_1$, thus $\mathbf{a}_1=\mathbf{d}(i)$.

3.4 Fault Mapping Procedure. Diagnostic reasoning in the ISM-Diagnostic method is based on matching the fault variation pattern (represented by eigenvalue/eigenvector pair obtained from the measurement data) against individual diagnostic vectors.

A statistical hypothesis test method is employed here to develop the decision criteria.

Let Σ represent the covariance matrix of $\mathbf{X}$ for the whole population, and ϖ_i's and $\mathbf{h}_i$'s be the eigenvalues and eigenvectors of Σ. Let λ_i's and $\mathbf{a}_i$'s be the corresponding eigenvalues and eigenvectors for the sample covariance matrix $\mathbf{S}$.

A hypothesis is formulated to test each diagnostic vector against the eigenvector that represents the fault pattern:

$$H_0: \quad \mathbf{h}_1=\mathbf{d}(i)$$

$$H_1: \quad \mathbf{h}_1\neq\mathbf{d}(i)$$

where $\mathbf{h}_1$ is the largest eigenvector of Σ that corresponds to the fault vector. $\mathbf{d}(i)$ is the ith diagnostic vector of the model.

According to the multivariate analysis theory [16], if the sampled eigenvector ϖ_i is a distinct root, the statistic $\mathbf{y}=(N-1)^{1/2}(\mathbf{a}_1-\mathbf{h}_1)$ follows a n-variate normal distribution of $N_n(\mathbf{0},\Gamma)$ (as $(N-1)\rightarrow\infty$), i.e.

$$\Gamma=\sum_{j=2}^{n}\frac{\varpi_i\varpi_j}{(\varpi_i-\varpi_j)^2}\mathbf{h}_j\mathbf{h}_j^T \tag{18}$$

where N is the sample size.

A test statistic can be formulated as

$$\Omega_i=(N-1)\left(\lambda_1\mathbf{d}(i)^T\mathbf{S}^{-1}\mathbf{d}(i)+\frac{1}{\lambda_1}\mathbf{d}(i)^T\mathbf{S}\mathbf{d}(i)-2\right) \tag{19}$$

and Ω_i follows χ^2_{n-1}. Details of derivation are provided in the Appendix.

If $\Omega_i>\chi^2_{(\alpha,n-1)}$, then we reject H_0. Here α represents the confidence level of the test. If we reject H_0, it indicates that this particular $\mathbf{d}(i)$ does not match the variation pattern of the faulted data.

4 Simulation Results

In order to illustrate the proposed diagnosis method, simulations were conducted for various hypothetical faults. The structure of the rear door frame of a truck body is modeled and diagnosed in this study. The simulation procedure is illustrated in Fig. 4.

Figure 5(a) shows that the rear door frame includes the header member and two side pillars. Two MLPs located on the side pillars are used to monitor the dimensional variation of the door frame. Figure 5(b) indicates the corresponding beam structure model of the rear door frame.

This beam structure model describes the following information:

(i) position and direction of locators in the fixture (by nodes 1, 2, 3, 6, 7 and 10);
(ii) part-to-part joints (by nodes 5 and 8);
(iii) measurement points (by nodes 4 and 9, representing MLP1 and MLP2 respectively);
(iv) potential structural faults are assumed to be at any joints.

The beam-based model is developed following the procedure of Section 2. The elements of the beam-based model are summarized in Table 1.

The stiffness of each beam member representing the part/subassembly of the rear door frame was simplified to uniformity in the simulation. The normalized diagnostic vectors of this structure are derived and shown in Table 2.

To verify the robustness of the diagnostic approach for the single-fault-at-a-time assumption, the noise/signal ratio is set to be 30 percent, which indicates that the dominant fault accounts for

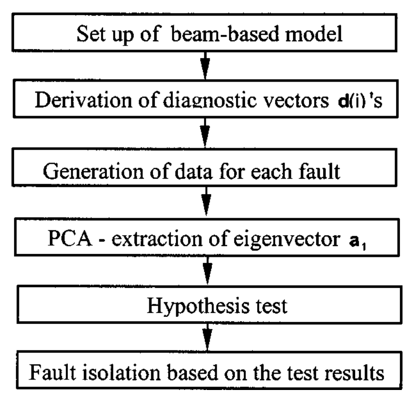

Fig. 4 The procedure for the conducted simulations

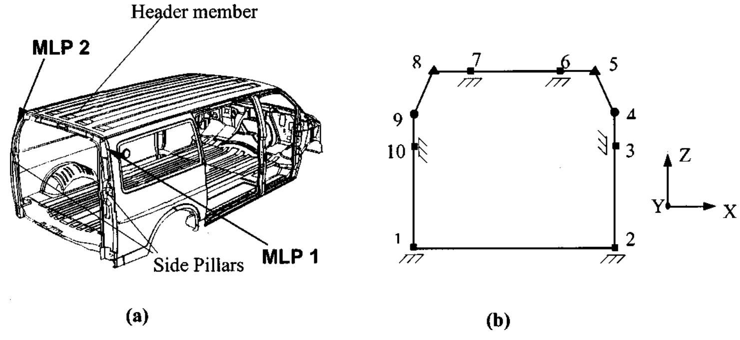

Fig. 5 The beam structure of the rear door opening

Table 1 The modeling elements of the beam structure of rear door frame

Location \ Type	Fixture locators	Joining points	MLPs
Node 1 (x,y,z)	X		
Node 2 (x,y,z)	X		
Node 3 (x)	X		
Node 6 (z)	X		
Node 7 (z)	X		
Node 10 (x)	X		
Node 5 (x,z)		X	
Node 8 (x,z)		X	
Node 4 (x)			X
Node 9 (x)			X

Table 2 The normalized diagnostic vectors for different hypothetical faults

Fault	at node 4 in X	at node 5 in X	at node 5 in Z	at node 8 in X	at node 8 in Z	at node 9 in X
	d(1)	**d**(2)	**d**(3)	**d**(4)	**d**(5)	**d**(6)
Diagnostic vector	$\begin{bmatrix}0.8592\\0.5116\end{bmatrix}$	$\begin{bmatrix}0.7671\\0.6416\end{bmatrix}$	$\begin{bmatrix}0.4200\\-0.9086\end{bmatrix}$	$\begin{bmatrix}0.6416\\0.7671\end{bmatrix}$	$\begin{bmatrix}0.9086\\-0.4200\end{bmatrix}$	$\begin{bmatrix}0.5116\\0.8592\end{bmatrix}$

Table 3 The eigenvectors for the simulated displacements

Fault	1	2	3	4	5	6
at	node 4 (x)	node 5 (x)	node 5 (z)	node 8 (x)	node 8 (z)	node 9 (x)
Eigen vector	$\begin{bmatrix}0.8744\\0.4853\end{bmatrix}$	$\begin{bmatrix}0.7750\\0.6319\end{bmatrix}$	$\begin{bmatrix}0.3202\\-.9473\end{bmatrix}$	$\begin{bmatrix}0.6467\\0.7627\end{bmatrix}$	$\begin{bmatrix}0.8899\\-.4561\end{bmatrix}$	$\begin{bmatrix}0.5067\\0.8522\end{bmatrix}$

Table 4 The hypothesis test results Ω_i for all simulated faults

Diagnostic vector	**d**(1)	**d**(2)	**d**(3)	**d**(4)	**d**(5)	**d**(6)
Fault 1	**1.59**	50.98	1417.40	183.88	929.41	359.78
Fault 2	16.35	**0.18**	719.06	27.36	619.23	89.62
Fault 3	369.92	336.29	**5.59**	281.91	205.27	223.36
Fault 4	159.01	43.81	1246.00	**0.12**	1406.40	41.28
Fault 5	434.99	514.03	231.88	576.59	**2.17**	603.61
Fault 6	618.81	301.78	1807.20	72.21	2650.20	**0.06**

70 percent of the total variation. The simulated data for hypothetical faults are assumed to be normally distributed.

PCA is performed based on the simulated structure displacements under hypothetical faults, and the eigenvectors (variation patterns) of the simulated data of all hypothetical faults are summarized in Table 3.

Hypothesis test is performed for each fault model. The test results for all of the simulated faults are summarized in Table 4.

In the structure used in the simulation, $n=2$. Let type I error $\alpha=0.01$, then $\chi^2_{(\alpha,n-1)}=\chi^2_{(0.01,1)}=6.63$. Fault 5 is used as an example to illustrate the test results. Based on the decision criteria, the test results for fault 5 indicate that **d**(1), **d**(2), **d**(3), **d**(4), and **d**(6) should be rejected. Since $\Omega_5=2.17<6.63$, we conclude that **d**(5) is the matching diagnostic vector of $\mathbf{a}_1$. From Table 2, we can find that diagnostic vector **d**(5) corresponds to fault at node 8 in Z direction.

Based on the proposed procedure, the diagnostic vector corresponding to each simulated structure fault can be isolated.

5 Case Study

The case study presented here is from the real production of a domestic automotive body assembly process [17].

The measurement point locations are the same as those described in Section 4, MLP1 and MLP2 on the rear doorframe (Fig. 5(*a*)). A large variation was observed in the X direction of the rear door opening. Figure 6 shows the in-line measurements at these two points.

The diagnostic vectors are the same as in Table 2. PCA analysis of the measurement data shows that the first variation pattern explains 95.2 percent of the total variation. The first eigenvalue is $\lambda_1=0.3569$, and the eigenvector corresponding to the 1st eigenvalue is $\mathbf{a}_1=[0.7398 \quad 0.6729]^T$.

Again, hypothesis tests for each diagnostic vector $\mathbf{d}(i)$ in Table 2 against the fault vector $\mathbf{a}_1$ are conducted. Set the type I error $\alpha=0.01$, $\chi^2_{(\alpha,n-1)}=\chi^2_{(0.01,1)}=6.63$. The test results are shown in Table 5.

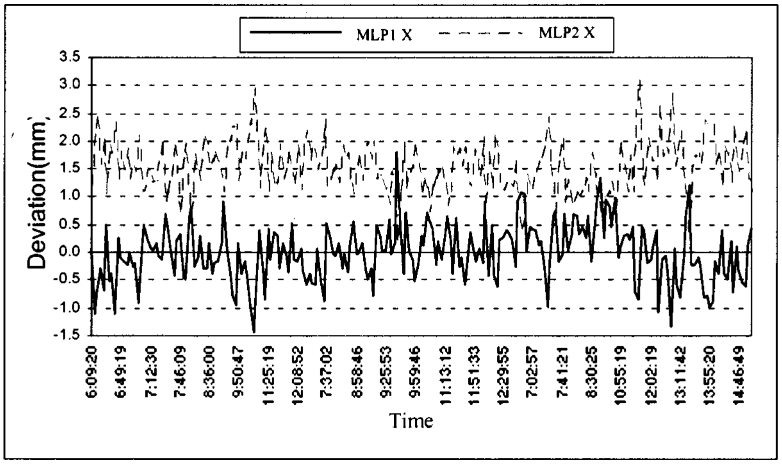

Fig. 6 The in-line measurement data of point MLP1 and MLP2 on the rear door opening

Table 5 The hypothesis test results for the diagnostic vectors

Diagnostic vector	$\mathbf{d}(1)$	$\mathbf{d}(2)$	$\mathbf{d}(3)$	$\mathbf{d}(4)$	$\mathbf{d}(5)$	$\mathbf{d}(6)$
Fault	at node 4 in X	**at node 5 in X**	at node 5 in Z	at node 8 in X	at node 8 in Z	at node 9 in X
Ω_i	71.29	**3.11**	1629.40	32.92	1519.90	151.64
$\chi^2_{(0.01,1)} = 6.63$	$\Omega_1 > \chi^2_{(0.01,1)}$	$\Omega_2 < \chi^2_{(0.01,1)}$	$\Omega_3 > \chi^2_{(0.01,1)}$	$\Omega_4 > \chi^2_{(0.01,1)}$	$\Omega_5 > \chi^2_{(0.01,1)}$	$\Omega_6 > \chi^2_{(0.01,1)}$

Diagnostic vector $\mathbf{d}(2)$ is concluded as the matching diagnostic vector of $\mathbf{a}_1$. From Table 2, diagnostic vector $\mathbf{d}(2)$ corresponds to node 5 in X direction. Therefore, it was diagnosed that fault 2 (at node 5 in X direction) was the root cause of the dimensional problem described by the analyzed data with confidence of 99 percent. The detailed investigation of the fixture in the manufacturing process confirmed the interference between the header panel and the right side pillar of the rear doorframe in the area of upper right corner (node 5; Fig. 5(*b*)) in the X direction.

6 Conclusion

The complexity of modern sheet metal assembly processes requires systematic in-process fault diagnostic methods for detection and isolation of dimensional faults considering the compliance characteristics of sheet metals. Such diagnostic methods need to be based on the comprehensive model of key process and product characteristics. Currently used diagnostic methodologies are based on the assumption of rigid parts and can diagnose only fixture-related faults (part misalignment during assembly process or lack of part location stability). This paper develops a diagnostic method for compliant assemblies based on the beam structure model and in-line measurements. The presented method is generic and can be applied to a general class of assembly processes of compliant parts.

The developed methodology allows the identification and isolation of dimensional faults of part-to-part interferences resulted from part fabrication errors in compliant assemblies. A generic analytical model of dimensional faults (variation patterns) for compliant beam structure assemblies is developed in the form of diagnostic vector based on the inversed stiffness matrix of the modeled beam structure. Fault variation patterns obtained from measurement data are modeled as eigenvalue/eigenvector pairs using principal component analysis. The analytical relationship between diagnostic vectors and fault variation patterns obtained is derived, which establishes the basis for the fault diagnosis. The mapping of unknown faults (eigenvalue/eigenvector pair) against a set of fault pattern models (diagnostic vectors) is developed based on statistical hypothesis tests. Simulations are performed to verify the developed approach. One case study based on real production data is presented. Both the simulation and the case study demonstrated that the dimensional faults can be isolated effectively by using this diagnostic approach.

Acknowledgment

This work was partially supported by the NSF CAREER award: DMI 9624402 and NSF Grant: DMI 9713654. The authors would also like to gratefully acknowledge the referees for their many insightful comments.

Appendix: Derivation of the Hypothesis Test Used in the Proposed Diagnostic Method

Let Σ represent the covariance matrix of measurements $\mathbf{X}$ for the whole population, and ϖ_i's and $\mathbf{h}_i$'s be the eigenvalues and eigenvectors of Σ. And let λ_i's and $\mathbf{a}_i$'s represent the corresponding eigenvalues and eigenvectors for the sample covariance matrix $\mathbf{S}$.

The test hypotheses are:

$$H_0: \quad \mathbf{h}_1 = \mathbf{d}(i)$$

$$H_1: \quad \mathbf{h}_1 \neq \mathbf{d}(i)$$

where $\mathbf{h}_1$ is the largest eigenvector of Σ that corresponds to the fault vector. $\mathbf{d}(i)$ is the *i*th diagnostic vector of the model.

From Muirhead [16], the sampled eigenvectors follow a certain distribution. If ϖ_i is a distinct root, then as $(N-1)\to\infty$, $(N-1)^{1/2}(\mathbf{a}_i-\mathbf{h}_i)$ follow n-variate normal distribution of $N_n(\mathbf{0},\Gamma)$, where

$$\Gamma = \varpi_i \sum_{\substack{j=1 \\ j\neq i}}^{n} \frac{\varpi_j}{(\varpi_i-\varpi_j)^2}\mathbf{h}_j\mathbf{h}_j^T$$

and N is the sample size.

Therefore, the distribution of $\mathbf{y}=(N-1)^{1/2}(\mathbf{a}_1-\mathbf{h}_1)$ is $N_n(\mathbf{0},\Gamma)$, where

$$\Gamma=\sum_{j=2}^{n}\frac{\varpi_i\varpi_j}{(\varpi_i-\varpi_j)^2}\mathbf{h}_j\mathbf{h}_j^T$$
$$=\mathbf{H}_2\mathbf{B}^2\mathbf{H}_2^T$$

with $\mathbf{H}_2=[\mathbf{h}_2,\ldots,\mathbf{h}_n]$ and

$$\mathbf{B}^2=\begin{bmatrix}\frac{\varpi_1\varpi_2}{(\varpi_1-\varpi_2)^2} & \vdots & \cdots & 0\\ \vdots & \frac{\varpi_1\varpi_3}{(\varpi_1-\varpi_3)^2} & \cdots & \vdots\\ \vdots & \vdots & \ddots & \vdots\\ 0 & \vdots & \cdots & \frac{\varpi_1\varpi_n}{(\varpi_1-\varpi_n)^2}\end{bmatrix},$$

Let $\mathbf{z}=\mathbf{B}^{-1}\mathbf{H}_2^T\mathbf{y}$, then the distribution of $\mathbf{z}$ is $N_{n-1}(\mathbf{0},\mathbf{I}_{n-1})$, $\mathbf{I}_{n-1}$ is the unit matrix with dimension of $n-1$. Hence the distribution of $\mathbf{z}^T\mathbf{z}$ is χ^2_{n-1}. Notice that since

$$\mathbf{z}^T\mathbf{z}=\mathbf{y}^T\mathbf{H}_2[\mathbf{B}^2]^{-1}\mathbf{H}_2^T\mathbf{y}$$

we can derive that

$$\mathbf{H}_2[\mathbf{B}^2]^{-1}\mathbf{H}_2^T=\varpi_1\Sigma^{-1}-2\mathbf{I}+\frac{1}{\varpi_1}\Sigma$$

Hence the distribution of

$$(N-1)(\mathbf{a}_1-\mathbf{h}_1)^T\left(\varpi_1\Sigma^{-1}-2\mathbf{I}+\frac{1}{\varpi_1}\Sigma\right)(\mathbf{a}_1-\mathbf{h}_1)$$
$$=(N-1)\left(\varpi_1\mathbf{a}_1^T\Sigma^{-1}\mathbf{a}_1+\frac{1}{\varpi_1}\mathbf{a}_1^T\Sigma\mathbf{a}_1-2\right)$$

is χ^2_{n-1}.

Since $\mathbf{S}$, $\mathbf{S}^{-1}$, and λ_1 are consistent estimates of Σ, Σ^{-1}, and ϖ_1, they can be substituted for Σ, Σ^{-1}, and ϖ_1 without affecting the distribution. Hence when the null hypothesis H_0: $\mathbf{h}_1=\mathbf{d}(i)$ is true, the distribution of

$$\Omega_i=(N-1)\left(\lambda_1\mathbf{d}(i)^T\mathbf{S}^{-1}\mathbf{d}(i)+\frac{1}{\lambda_1}\mathbf{d}(i)^T\mathbf{S}\mathbf{d}(i)-2\right)$$

is χ^2_{n-1}.

References

[1] Mo, K. J., Lee, G., Nam, D. S., Yoon, Y. H., and Yoon, E. S., 1997, ''Robust Fault Diagnosis Based on Clustered System Trees,'' Control Eng. Practice, **5**, No. 2, pp. 199–208.

[2] Pau, L. F., 1975, *Failure Diagnosis and Performance Monitoring*, Marcel Dekker, New York, NY.

[3] Danai, K., and Chin, H., 1991, ''Fault Diagnosis with Process Uncertainty,'' ASME J. Dyn. Syst., Meas., Control, **113**, pp 339–343.

[4] Ceglarek, D., Shi, J., and Wu, S. M., 1994, ''A Knowledge-Based Diagnosis Approach for the Launch of the Auto-Body Assembly Process,'' ASME J. Eng. Ind., **116**, No. 3, pp. 491–499.

[5] Ceglarek, D., and Shi, J., 1996, ''Fixture Failure Diagnosis for Autobody Assembly Using Pattern Recognition,'' ASME J. Eng. Ind., **118**, No. 2, pp. 55–66.

[6] Apley, D., and Shi, J., 1998, ''Diagnosis of Multiple Fixture Faults in Panel Assembly,'' ASME J. Manuf. Sci. Eng., **120**, No. 4, pp. 793–801.

[7] Rong, Y., and Bai, Y., 1996, ''Machining Accuracy Analysis for Computer-Aided Fixture Design and Verification,'' ASME J. Manuf. Sci. Eng., **118**, No. 8, pp. 289–300.

[8] Jin, J., and Shi, J., 1999, ''State Space Modeling of Sheet Metal Assembly for Dimensional Control,'' ASME J. Manuf. Sci. Eng., **121**, No. 4, pp. 756–762.

[9] Shalon, D., Gossard, D., Ulrich, K., Fitzpatrick, D., 1992, ''Representing Geometric Variations in Complex Structural Assemblies on CAD Systems,'' Adv. Des. Autom., **2**, pp. 121–132.

[10] Shiu, B., Ceglarek, D., and Shi, J., 1997, ''Flexible Beam-Based Modeling of Sheet Metal Assembly for Dimensional Control,'' Trans. of NAMRI, **XXV**, pp. 49–54.

[11] Ceglarek, D., and Shi, J., 1995, ''Dimensional Variation Reduction for Automotive Body Assembly,'' *Manufacturing Review*, Vol. 8, No. 2, pp. 139–154.

[12] Ceglarek, D., and Shi, J., 1998, ''Design Evaluation of Sheet Metal Joints for Dimensional Integrity,'' ASME J. Manuf. Sci. Eng., **120**, No. 2, pp. 452–460.

[13] Chon, C. T., Mohammadtorab, H., and EI-Essawi, M., 1986, ''Generic Stick Model of a Vehicular Structure,'' SAE Paper 860825.

[14] West, H., 1989, *Analysis of Structure: An Integration of Classical and Modern Methods*, Wiley, New York.

[15] Mackiewicz, A., and Ratajczak, W., 1993, ''Principal Component Analysis (PCA),'' Comput. Geosci., **19**, No. 3, pp. 303–342.

[16] Muirhead, R., 1982, *Aspects of Multivariate Statistical Theory*, Wiley.

[17] Rong, Q., Ceglarek, D., and Shi, J., 1997, ''Dimensional Variation Reduction for Automotive Body Assembly: Evaluation of Tooling Design and Process Design,'' Technical Report of the ''2 mm'' Program, University of Michigan, Ann Arbor.